are the ones which predominantly control the solution behavior of these systems.

In agreement with Overbergh et al.,[21] we have determined that the IPS gel crystals consist of a high-energy conformational variant of the usual isotactic configuration. The normal 4_1 helical tetragonal form of PPO was found in its gel crystals. Crystal size and perfection and microphase separation in glasses of PS, PPO, and their blends cast from gel solutions were affected by gelation solvent and annealing treatment.

The microheterogeneities within these glasses should have a significant effect upon plastic microdeformation morphology. With the structural characterization of these materials in hand, subsequent reports will attempt to explore structure–property relationships of these materials. The "critical" microheterogeneity size responsible for crazing and localized microshear banding will be of special interest.

Acknowledgment. The authors wish to acknowledge support of this work by the NSF through Grant DMR 76-80710-A01. Special thanks are due to Professor Andrew Keller who initially encouraged us to study this problem and who since has made many valuable suggestions. We would also like to acknowledge the helpful discussions we had with Professor Paul Painter on the interpretation of the FTIR results on IPS gels.

References and Notes

(1) J. W. Cahn, *J. Chem. Phys.*, **42** (1), 93 (1965); *Trans. Am. Inst. Min., Metall. Pet. Eng.*, **242**, 166 (1968).
(2) L. D. Grandine and J. Ferry, *J. Appl. Phys.*, **24** (6), 679 (1953).
(3) A. A. Tager, V. E. Dreval, M. S. Lutsky, and G. V. Vinogradov, *J. Polym. Sci., Part C*, **23**, 181 (1968).
(4) M. Girolamo, A. Keller, K. Miyasaka, and N. Overbergh, *J. Polym. Sci., Polym. Phys. Ed.*, **14**, 39 (1976).
(5) D. R. Paul, *J. Appl. Polym. Sci.*, **11**, 439 (1967).
(6) G. S. Y. Yeh, *Crit. Rev. Macromol. Sci.*, **1** (2), 1973 (1972).
(7) "Polymer Handbook", J. Brandup and E. H. Immergut, Eds., Wiley, New York, 1975.
(8) P. J. Flory, "Principles of Polymer Chemistry", Interscience, New York, 1953.
(9) Y. Izumi and Y. Miyake, *Polym., J.*, **3**, 647 (1972).
(10) C. M. Hansen, *J. Paint Technol.*, **39** (505), 104 (1967).
(11) S. H. Maron and F. E. Filisko, *J. Macromol. Sci., Phys.*, **6**, 57 (1970).
(12) M. Kobayashi, K. Tsumura, and H. Tadokoro, *J. Polym. Sci., Part A-2*, **6**, 1493 (1978).
(13) M. Kobayashi, K. Akita, and H. Tadokoro, *Makromol. Chem.*, **118**, 324 (1968).
(14) G. Natta, P. Corradini, and I. W. Bassi, *Nuovo Cimento, Suppl.*, **15**, 68 (1960).
(15) S. Wellinghoff and Eric Baer, to be published.
(16) P. Painter and J. L. Koenig, *J. Polym. Sci., Polym. Phys. Ed.*, **15** (11), 1885 (1977).
(17) E. D. Atkins, D. H. Isaac., A. Keller, and K. Miyasaka, *J. Polym. Sci., Polym. Phys. Ed.*, **15**, 211 (1977).
(18) J. M. Barrales-Rienda and J. M. G. Fatou, *Kolloid Z. Z. Polym.*, **244**, 317 (1971).
(19) A. Factor, G. E. Heinshon, and L. H. Vogt, Jr., *J. Polym. Sci., Part B*, **7**, 205 (1969).
(20) S. Wellinghoff, J. L. Koenig, and Eric Baer, *J. Polym. Sci., Polym. Phys. Ed.*, **15** (11), 1913 (1977).
(21) N. Overbergh and H. Berghmans, *Polymer*, **18**, 883 (1977).
(22) S. Wellinghoff and Eric Baer, *J. Appl. Polym. Sci.*, **22**, 2025 (1978).
(23) "International Critical Tables", Vol. 5, 1929, p 157.
(24) R. Foster, "Organic Charge-Transfer Complexes", Academic Press, New York, 1969.

Fast Neutron Irradiation Effects on Polymers. 1. Degradation of Poly(methyl methacrylate)

Shigenori Egusa,[1] Kenkichi Ishigure, and Yoneho Tabata*

Nuclear Engineering Research Laboratory, The University of Tokyo, Tokai-mura, Ibaraki 319-11, Japan. *Received April 10, 1979*

ABSTRACT: Irradiation effects of fast neutrons on poly(methyl methacrylate) were compared with those of ^{60}Co γ rays from the viewpoint of linear energy transfer (LET). The G value of main-chain scissions, G(S), and the change in the molecular weight distribution of irradiated polymers were determined by means of gel-permeation chromatography. The LET dependence of G(S) is definite for in-vacuo irradiations [$G\gamma^{vacuo}$(S) = 1.54 ● 0.11 for ^{60}Co γ rays (LET: ca. 0.02 eV/Å) and G_n^{vacuo}(S) = 1.04 ± 0.13 for fast neutrons (LET: ca. 3.7 eV/Å)], but the dependence is not so definite for in-air irradiations [G_γ^{air}(S) = 0.73 ± 0.06 and G_n^{air}(S) = 0.66 ± 0.10]. The plot of the M_w/M_n ratio vs. the number of main-chain scissions deviates from that predicted by the random-degradation theory. The deviation is more distinct for fast-neutron than for γ-ray irradiations. The reduced G(S) value and the enhanced deviation from the random degradation at high LET are attributable to the increased inhomogeneity of microscopic energy deposition. A parameter expressing the microscopic inhomogeneity, $\Delta D/x$, is introduced in the computer simulation of the nonrandom degradation and is adjusted so as to give the best fit between the observed and simulated plots of the M_w/M_n change. The computer simulation gives the $\Delta D/x$ value of 1.54 and 0.52 Mrad for fast-neutron and γ-ray irradiations, respectively, indicating that the $\Delta D/x$ ratio (ca. 3) is strikingly small compared with the LET ratio (ca. 180).

Fast-neutron and ^{60}Co γ-ray irradiations on polymers will produce different effects not only in the efficiency of main-chain scission, cross-linking, etc., but also in the molecular weight distribution change. The different effects are considered to arise from a difference in linear energy transfer (LET) between recoil protons and secondary electrons which are produced by the interaction of atoms with fast neutrons and γ rays, respectively. The LET difference will produce differences in the spatial distribution of energy deposition[2,3] and, consequently, in the spatial distribution of reactive species such as macroradicals and low molecular weight free radicals. Several authors have carried out the ESR study on the spatial distribution of free radicals trapped in matrices such as poly(methyl methacrylate) (PMMA),[4,5] glassy methanol,[6] and *n*-eicosane single crystal[7,8] irradiated with different types of radiation such as protons from an accelerator and ^{60}Co γ rays. Kaul and Kevan[5] found that the local spin

0024-9297/79/2212-0939$01.00/0

concentration of radicals trapped in a PMMA matrix is definitely higher for proton than for γ-ray irradiation and that the concentration ratio is 5.9.

When polymers are irradiated with high LET radiations, ionization and/or excitation may occur at the same time at several segments of the same chain.[9] This probability is expected to increase with increasing LET and molecular size of polymers. The multi-ionization or excitation of the same chain, therefore, will produce the observable LET effects not only on the yields of scission, cross-linking, and gaseous products but also on the molecular weight distribution changed by scission and cross-linking. Furthermore, the multi-ionization or excitation will invalidate the assumption that the main-chain scission and cross-linking take place at random, which has been made both in the theory of changes in molecular weight distribution[10-18] and in the evaluation of the G values.[19-26]

From these points of view, we studied the G value of scission or cross-linking and the molecular weight distribution change in ^{60}Co γ-ray and fast-neutron irradiated polymers such as PMMA and polystyrene and were able to find the definite LET effects caused by the two types of radiation.[27] The present paper mainly describes the LET effects observed for PMMA and the results of computer simulation which was made by taking into consideration the inhomogeneity of energy deposition in order to explain the nonrandom degradation observed especially in fast-neutron irradiated PMMA. A later paper of this series[28] will describe the LET effects observed for the degradation and cross-linking of polystyrene and the results of computer simulation made on the same basis as that mentioned for PMMA.

Experimental Section

(1) Irradiation Procedures. Commercial PMMA powder was purified by fractional precipitation, using benzene as solvent and methanol as precipitant. The tacticity of this polymer was shown to be mainly heterotactic by the NMR measurement. Polyethylene capsules were used for in-air irradiations. For in-vacuo irradiations, capsules made of quartz and Pyrex glass were used for fast-neutron and γ-ray irradiations, respectively. These capsules were evacuated until the pressure decreased below 10^{-5} torr.

The γ-ray irradiations were made with a ^{60}Co source at room temperature or 60 °C at a dose rate of 0.22 or 1.80 Mrad/h. No effect of irradiation temperature and dose rate was observed under the present experimental conditions. The fast-neutron irradiations were made with the fast-neutron research reactor YAYOI.[29] Samples were inserted into the irradiation hole (called "Glory hole") which penetrates the reactor core made of enriched uranium. The reactor power was set at 500 W during the irradiation. A copper–constantan thermocouple attached to the capsule showed the sample temperature to be kept below 33 °C under the present irradiation conditions.

(2) Absorbed Dose Measurements. The dose rate of the ^{60}Co γ-ray source used here was determined according to the usual procedures of the Fricke and ceric sulfate dosimeters. For in-reactor irradiations, the dose rates due to fast neutrons and the concomitant γ rays have to be estimated separately. We tried to use the four combinations of the Fricke and ceric sulfate dosimeters of water and heavy water for this purpose and were able to prove these combinations of dosimeters to be useful as a simple and accurate method. The details are described in a previous paper.[30] According to the result, the dose rates due to fast neutrons and the concomitant γ rays in PMMA inserted into the Glory hole are 1.31 (86%) and 0.22 Mrad/h (14%), respectively, at the reactor power of 500 W.

(3) Measurements of Molecular Weight Distributions. Measurements of molecular weight distributions were carried out with a gel-permeation chromatography (GPC) apparatus of Waters Associates Inc. This apparatus was equipped with a differential refractometer detector and five series-connected fractionating columns packed with styragel beads of 10^6, 10^5, 10^4, 10^3, and 500 Å nominal porosities. A ca. 0.5% PMMA solution in tetrahydrofuran (THF) was injected into the THF mobile phase of 2 mL/min flow rate at room temperature.

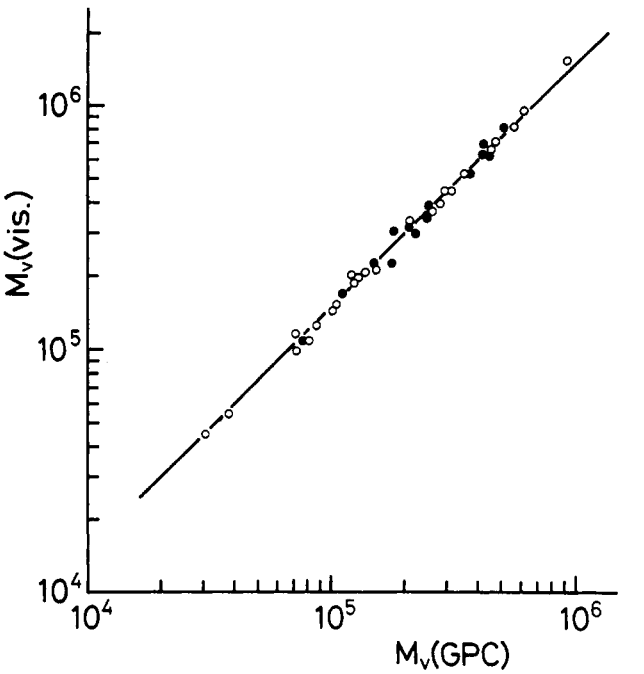

Figure 1. Correlation between viscometrically-derived and GPC-derived viscosity-average molecular weights, M_v(vis.) and M_v(GPC), for PMMA irradiated with ^{60}Co γ rays (○) and fast neutrons (●).

The number- and weight-average molecular weights, M_n and M_w, were calculated from the GPC chromatograms by using the calibration curve for PMMA, which was determined in the following way. The calibration curve for polystyrene was tentatively used to convert the GPC chromatogram of PMMA to the viscosity-average molecular weight, M_v(GPC), by

$$M_v(\mathrm{GPC}) = \left[\frac{\sum H_i (M_i)^{0.76}}{\sum H_i} \right]^{1/0.76} \quad (1)^{31}$$

where H_i is the height of the chromatogram at equally spaced intervals along the elusion volume axis, and M_i is the molecular weight of polymers having the same elusion volume as when the H_i value is taken. The intrinsic viscosity of PMMA in benzene at 30 °C, $[\eta]$, was also measured and converted to the viscosity-average molecular weight, M_v(vis.), by

$$M_v(\mathrm{vis.}) = ([\eta]/5.2 \times 10^{-5})^{1/0.76} \quad (2)^{32}$$

The correlation between M_v(vis.) and M_v(GPC) is shown in Figure 1 for PMMA before and after irradiations with ^{60}Co γ rays and fast neutrons and is seen to be expressed by M_v(vis.) = 1.50 × M_v(GPC). The GPC calibration curve for PMMA, accordingly, was determined to be 1.50 times the molecular weight axis of the calibration curve for polystyrene.

Results

(1) G Value of Main-Chain Scissions. Figure 2 shows typical examples of the GPC chromatograms obtained for PMMA before irradiation (dotted curve) and after in-vacuo irradiations in the ^{60}Co γ-ray source (broken curve) and in the nuclear reactor (solid curve). Comparison of the chromatogram before irradiation with that after irradiation with γ rays or fast neutrons demonstrates that main-chain scission occurs predominantly for both types of radiation, although the possibility of concurrent cross-linking has been suggested for PMMA.[24] Consequently, the G value of main-chain scissions, G(S), can be evaluated from the following equation[10] which has been derived on the assumption of random degradation that all monomer units

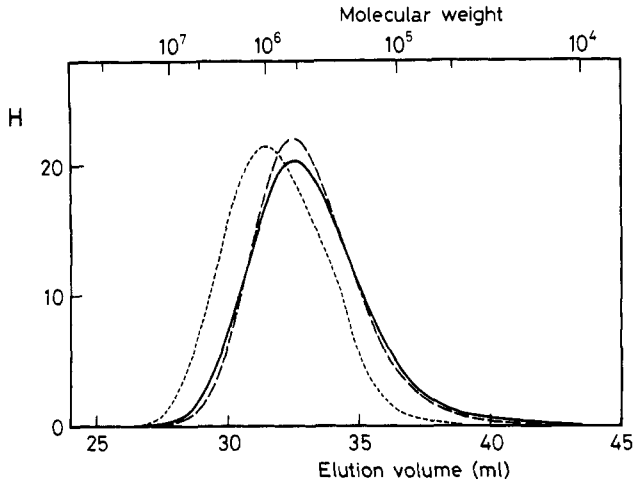

Figure 2. GPC chromatograms for PMMA before irradiation (dotted curve) and after in-vacuo irradiations in a ^{60}Co γ-ray source to the $u\tau$ value of 0.94 (broken curve) and in the fast-neutron reactor to the $u\tau$ value of 0.97 (solid curve). See text for $u\tau$.

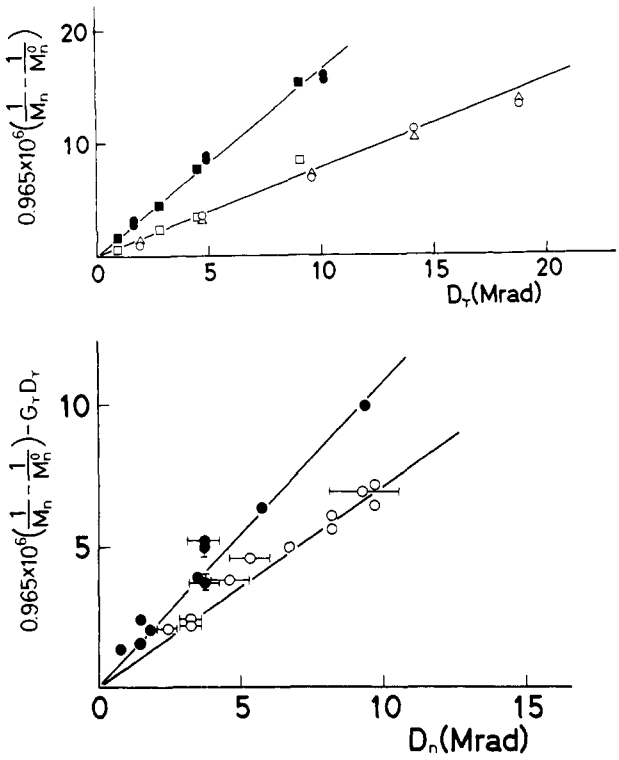

Figure 3. Plot of the number of main-chain scissions vs. the absorbed dose D_γ due to ^{60}Co γ rays (a, top) and D_n due to fast neutrons (b, bottom). For (b), corrections are made for the concomitant γ rays by the term of $G_\gamma D_\gamma$ (see text). The open (○, △, □) and solid points (●, ■) are the data for in-air and in-vacuo irradiations, respectively: (○, ●) at room temperature, at a dose rate of 0.22 Mrad/h for (a) and below 33 °C and 1.53 Mrad/h for (b); (△) at 60 °C and 0.22 Mrad/h; (□, ■) at room temperature and 1.80 Mrad/h.

have the same probability of bond rupture during irradiation:

$$0.965 \times 10^6\left(\frac{1}{M_n} - \frac{1}{M_n^0}\right) = G(S)D \qquad (3)$$

where M_n^0 is the number-average molecular weight before irradiation ($M_n^0 = 8.07 \times 10^5$ for PMMA used in the present work), and D is the absorbed dose in Mrad. The M_n change by irradiation depends only on the number of main-chain scissions and not on the spatial distribution

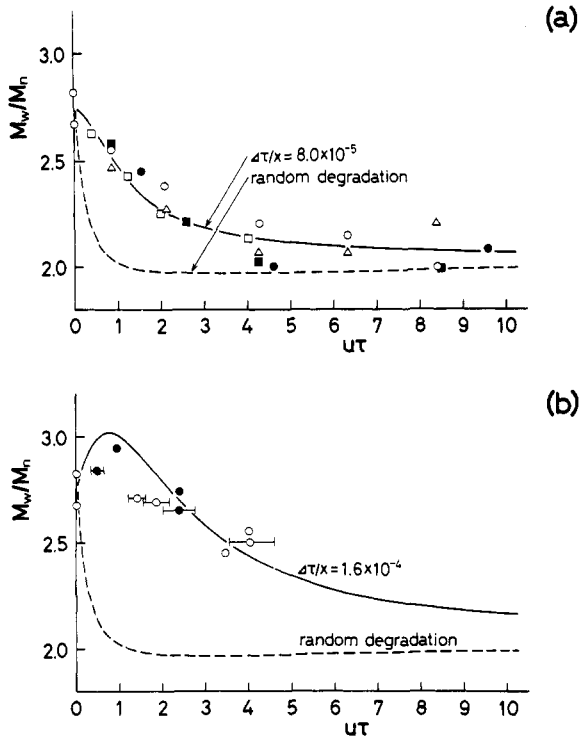

Figure 4. Plot of the M_w/M_n ratio vs. the number of main-chain scissions per initial number-average molecule, $u\tau$, due to ^{60}Co γ rays (a) and fast neutrons (b). For the open and solid points such as ○ and ●, see the caption for Figure 3. The broken and solid curves are the results of computer simulation made for the random and nonrandom degradation, respectively. See the text for $\Delta\tau/x$.

of the scissions. Equation 3, therefore, holds not only for the random degradation but also for the nonrandom degradation which is expected to occur especially for high LET radiations such as fast neutrons.

Figure 3a shows the plots of the left-hand side of eq 3 vs. D for ^{60}Co γ-ray irradiations. The slopes of these linear plots and the least-squares method gave the following $G(S)$ values and the 95% confidence limits, $G_\gamma^{vacuo}(S) = 1.54 \pm 0.11$ and $G_\gamma^{air}(S) = 0.73 \pm 0.06$ for in-vacuo and in-air γ irradiations, respectively.

For in-reactor irradiations, eq 3 is modified into the following equation in order to estimate the $G(S)$ value due to fast neutrons separating due to γ rays in the reactor:

$$0.965 \times 10^6\left(\frac{1}{M_n} - \frac{1}{M_n^0}\right) - G_\gamma(S)D_\gamma = G_n(S)D_n \qquad (4)$$

where the subscripts γ and n represent the γ-ray and fast-neutron contributions, respectively. Since the absorbed dose due to γ rays in the reactor, D_γ, is known,[30] the left-hand side of this equation can be evaluated by assuming that the $G_\gamma(S)$ value due to γ rays in the reactor is the same as that due to ^{60}Co γ rays. Figure 3b shows the plots of the left-hand side of eq 4 vs. the absorbed dose due to fast neutrons, D_n. The $G(S)$ values due to fast neutrons were determined to be $G_n^{vacuo}(S) = 1.04 \pm 0.13$ and $G_n^{air}(S) = 0.66 \pm 0.10$ for in-vacuo and in-air irradiations, respectively.

(2) Change in Molecular Weight Distribution. Comparison of the GPC chromatograms of PMMA after irradiation (solid and broken curves in Figure 2) demonstrates that the molecular weight distribution of PMMA irradiated with fast neutrons is slightly but definitely broader than that with γ rays. Usually, the broadness of the molecular weight distribution is expressed by the M_w/M_n ratio. The M_w/M_n ratio is plotted in Figure 4 as

a function of the number of main-chain scissions per initial number-average molecule, $u\tau$, which is related to the absorbed dose D by

$$u\tau = \frac{M_n^0}{0.965 \times 10^6} G(S)D \quad (5)$$

For γ-ray irradiation (Figure 4a), the M_w/M_n ratio is found to decrease monotonously and to approach 2.0 as $u\tau$ increases. For fast-neutron irradiation (Figure 4b), on the other hand, the M_w/M_n ratio appears to increase at first and then decreases slowly with $u\tau$. Furthermore, the M_w/M_n ratio is always higher for fast neutrons than for γ rays at each $u\tau$ value. These characteristics of the M_w/M_n change with $u\tau$ are not affected by the irradiation conditions such as the atmosphere around the sample, dose rate, and temperature, except the type of radiation. It is concluded, therefore, that the characteristics of the M_w/M_n change observed here arise from the difference in the type of radiation.

Discussion

(1) LET Dependence of $G(S)$. The energy spectrum of recoil protons depends on that of fast neutrons incident upon a material. Fission neutrons, which are available in the reactor core used here, have the average energy of ca. 2 MeV, and the corresponding average energy of recoil protons is ca. 0.6 MeV.[30] The LET for the recoil protons of this energy in PMMA is ca. 3.7 eV/Å, while that for ^{60}Co γ rays is ca. 0.02 eV/Å.[33] The significant difference in LET suggests that the spatial distribution of energy deposition and the resulting reactive species is much more inhomogeneous along the tracks of fast neutrons than γ rays.

Our $G(S)$ values obtained for in-vacuo irradiation are $G_\gamma^{vacuo}(S) = 1.54 \pm 0.11$ and $G_n^{vacuo}(S) = 1.04 \pm 0.13$, and those for in-air irradiation are $G_\gamma^{air}(S) = 0.73 \pm 0.06$ and $G_n^{air}(S) = 0.66 \pm 0.10$. This result leads to the conclusion that the $G(S)$ value is appreciably decreased by the increase in LET for in-vacuo irradiation, whereas for in-air irradiation it is almost independent of LET within the experimental error. This LET dependence of $G(S)$ can be explained qualitatively both by the above-mentioned difference in the spatial distribution of reactive species and by the following reactions which were confirmed by the pulse radiolysis study on the degradation kinetics of PMMA in solution:[34]

$$P^*_{n+m} \rightarrow P_n + P_m \quad (6)$$

$$P\cdot_{n+m} \rightarrow P_n + P\cdot_m \quad (7)$$

$$P\cdot_{n+m} + S \rightarrow P_{n+m}\cdots S\cdot \text{ or } P_{n+m} + S\cdot \quad (8)$$

where P^*_{n+m} designates an excited or ionic species which dissociates rapidly into two macromolecules (reaction 6), and $P\cdot_{n+m}$ is a long-lived side-group macroradical which either dissociates spontaneously[35,36] (reaction 7) or is repaired by the reaction with a radical scavenger S such as oxygen (reaction 8). These reactions will occur for PMMA in solid also. For in-air irradiation, main-chain scission occurs only by the dissociation of P^*_{n+m} (reaction 6) because that of $P\cdot_{n+m}$ is inhibited by the reaction with oxygen (reaction 8). Since the dissociation of P^*_{n+m} is a unimolecular reaction, the main-chain scission by this reaction is expected not to depend on LET with respect to the number of scissions aside from its spatial distribution. This expectation is in accord with our result that the $G(S)$ value is almost independent of LET for in-air irradiations. For in-vacuo irradiations, on the other hand, main-chain scission occurs by the dissociation of $P\cdot_{n+m}$ (reaction 7) also, resulting in the increased $G(S)$ value compared with that for in-air irradiation. The increase in $G(S)$ will depend on the competition between the dissociation of $P\cdot_{n+m}$ and the repair by the reaction with a radical scanvenger (reaction 8). In this case of in-vacuo irradiation, the scavengers will be free radicals such as hydrogen atom, $\cdot CH_3$, and $\cdot OCH_3$ radicals, which are known to be produced in irradiated PMMA.[37-39] Since the repair of $P\cdot_{n+m}$ is a bimolecular reaction, it will be favored at high LET where $P\cdot_{n+m}$ and these free radicals of low molecular weight are produced so closely as to react with one another. Consequently, the increase in $G(S)$ is expected to be smaller for fast-neutron than for γ-ray irradiation. This expectation is in accord with our result that the increase in $G(S)$ is 0.81 for γ rays, whereas for fast neutrons it is merely 0.38.

(2) LET Dependence of Change in Molecular Weight Distribution. Saito[10] has derived the following formula for the molecular weight distribution of polymers undergoing random degradation:

$$m(p,\tau) = \left\{m(p,0) + 2\tau \int_p^\infty m(p,0)\, dp + \tau^2 \int_p^\infty dp \int_p^\infty m(p,0)\, dp\right\} e^{-p\tau} \quad (9)$$

where the degree of polymerization p is treated as continuous, $m(p,\tau)$ represents the molecular size distribution when the probability of bond rupture per monomer unit is increased up to τ, and $m(p,0)$ is the initial distribution which is normalized so as to become unity when integrated over p from zero to infinity. The νth moment of the distribution $m(p,\tau)$, $f_\nu(\tau)$, is defined by

$$f_\nu(\tau) = \int_0^\infty p^\nu m(p,\tau)\, dp \quad (\nu \geq 0) \quad (10)$$

For $\nu = 0$, 1, and 2, this equation becomes

$$f_0(\tau) = 1/u + \tau \quad (11)$$

$$f_1(\tau) = 1 \quad (12)$$

$$f_2(\tau) = \frac{2}{\tau} - \frac{2}{\tau^2}\int_0^\infty (1 - e^{-p\tau}) m(p,0)\, dp \quad (13)$$

where u stands for the initial number-average degree of polymerization. The M_w/M_n ratio as a function of τ

$$M_w/M_n = f_0(\tau) f_2(\tau) \quad (14)$$

can be calculated by using the GPC chromatogram of PMMA before irradiation (dotted curve in Figure 2) as the initial distribution $m(p,0)$ and is shown by the broken curve in Figures 4a or 4b as a function of $u\tau$, i.e., the number of scissions per initial number-average molecule. It is apparent that the calculated curve gives a fit neither to the observed points of M_w/M_n for γ irradiation (Figure 4a) nor to those for fast-neutron irradiation (Figure 4b) and that the discrepancy is more distinct for fast-neutron than for γ-ray irradiation. This finding suggests that the actual degradation of PMMA does not take place at random even for γ-ray irradiation as well as for fast-neutron irradiation.

The assumption of random degradation holds only when the radiation energy is deposited in a polymer homogeneously on both macroscopic and microscopic scales. The macroscopic homogeneity of energy deposition is easily obtainable since the mean free path of fast neutrons or γ rays in PMMA is of the order of a few centimeters. The microscopic energy deposition, on the other hand, is essentially inhomogeneous according to the track model proposed by Mozumder and Magee.[2,3] In this model, the energy deposition is made in the form of spurs, blobs, and short tracks for γ rays and in the form of cores composed of overlapping spurs for fast neutrons. The microscopic

inhomogeneity of energy deposition will cause degradation to proceed more rapidly than the random degradation in certain localized regions of PMMA at the expense of degradation in the other regions, making the molecular weight distribution broader than that predicted by the random degradation theory. Accordingly, this microscopic inhomogeneity is considered to be responsible for the nonrandom degradation of PMMA.

In order to confirm this view and to estimate the degree of the microscopic inhomogeneity of energy deposition, we carried out the computer simulation. When the total absorbed dose in a polymer system is increased by ΔD, let the increment be absorbed exclusively in a small part whose fraction to the whole system is x. In this case, the increment of absorbed dose within the small part becomes $\Delta D/x$, which is taken as a parameter expressing the degree of the microscopic inhomogeneity of energy deposition. We assume further that this process of energy deposition has been repeated independently N time when the total dose in the whole system is D, i.e., $D = \Delta DN$. When $x \ll 1$ and $\Delta D \ll D$, the following Poisson distribution gives the probability that the absorbed dose within the small part of x is $k\Delta D/x$:

$$P(k,\mu) = \mu^k e^{-\mu}/k! \tag{15}$$

where μ is the mean value of the Poisson distribution, i.e., $\mu = Nx$ or $D/(\Delta D/x)$.

The computer simulation was made by using τ and $\Delta\tau/x$ in place of D and $\Delta D/x$, respectively, with the relationships expressed by eq 5 and

$$\Delta\tau/x = \frac{w}{0.965 \times 10^6} G(\mathrm{S})\Delta D/x \tag{16}$$

where w is the molecular weight of the monomer unit. The molecular size distribution $m'(p,\tau)$ and the νth moment $f_\nu'(\tau)$ when the above-mentioned process is repeated independently N times ($N = \tau/\Delta\tau$) can be calculated from the following equations on the assumption that the degradation within the small part of x is at random:

$$m'(p,\tau) = \sum_{k=0}^{N} P(k,\tau/(\Delta\tau/x))m(p,k\Delta\tau/x) \tag{17}$$

$$f_\nu'(\tau) = \sum_{k=0}^{N} P(k,\tau/(\Delta\tau/x))f_\nu(k\Delta\tau/x) \tag{18}$$

where $m(p,k\Delta\tau/x)$ and $f_\nu(k\Delta\tau/x)$ are calculated from eq 9 and 10, respectively. For $\nu = 0$ and 1, substitution of eq 11 and 12 into 18 gives

$$f_0'(\tau) = 1/u + \tau \tag{19}$$

$$f_1'(\tau) = 1 \tag{20}$$

indicating that neither $f_0'(\tau)$ nor $f_1'(\tau)$ depend on the parameter $\Delta\tau/x$. However, both $m'(p,\tau)$ and $f_2'(\tau)$ depend on the $\Delta\tau/x$ value. For various values of $\Delta\tau/x$, for this reason, we calculated the M_w/M_n ratio from $f_0'(\tau)f_2'(\tau)$ as a function of τ and then tried to find the $\Delta\tau/x$ value which gives the best fit between the calculated and observed plots of M_w/M_n vs. $u\tau$. The best fit was found to be obtained when the $\Delta\tau/x$ value is adjusted to 8.0×10^{-5} and 1.6×10^{-4} for γ-ray and fast-neutron irradiations, respectively, as shown by the solid curves in Figure 4. This result confirms our view that the nonrandom degradation of PMMA is caused by the microscopic inhomogeneity of energy deposition.

The $\Delta D/x$ value is 0.52 and 1.54 Mrad for PMMA irradiated in vacuo with γ rays and fast neutrons, respectively, as evaluated from eq 16. Although the $\Delta D/x$ value is expected to be closely related to the LET value, the ratio for fast neutrons to γ rays ($1.54/0.52 \approx 3$) is strikingly small compared with the LET ratio ($3.7/0.02 \approx 180$). The small ratio of $\Delta D/x$ is compatible with the report that the local spin concentration of radicals trapped in PMMA differs only by a factor of 5.9 between proton and γ-ray irradiations.[5] These phenomena are considered to occur mainly because these overall LET values express merely the mean value of energy loss per unit distance along the track of ionizing radiations and hence do not necessarily reflect the microscopic distribution of energy deposition. According to the track model proposed by Mozumder and Magee,[2] even a track due to an ionizing particle of low overall LET has a kind of high LET component through the short tracks composed of overlapping spurs, where the instantaneous LET is much higher than the overall LET value. The high LET component for the low LET radiations such as γ rays may be responsible for the small difference in the $\Delta D/x$ value between γ-ray and fast-neutron irradiations compared with that in LET. Therefore, the parameter $\Delta D/x$ rather than LET is expected to reflect the actual degree of the microscopic inhomogeneity of energy deposition.

Acknowledgment. The authors wish to express their appreciation to Dr. Seiichi Tagawa and the operating staff of the fast-neutron research reactor YAYOI for their cooperation in carrying out the irradiations.

References and Notes

(1) Japan Atomic Energy Research Institute, Takasaki Radiation Chemistry Research Establishment, Takasaki-shi, Gumma 370-12, Japan.
(2) A. Mozumder and J. L. Magee, *Radiat. Res.*, **28**, 203 (1966); *J. Chem. Phys.*, **45**, 3332 (1966).
(3) A. Mozumder, A. Chatterjee, and J. L. Magee, *Adv. Chem. Ser.*, **No. 81** (1968).
(4) W. Kaul and L. Kevan, *J. Phys. Chem.*, **75**, 2443 (1971).
(5) W. Kaul and L. Kevan, *Proc. Tihany Symp. Radiat. Chem., 3rd.*, **1**, 919 (1972).
(6) A. M. Raitsimring, Yu. D. Tsvetkov, and V. M. Moraev, *Int. J. Radiat. Phys. Chem.*, **5**, 249 (1973).
(7) K. Hamanoue, V. Kamatauskas, Y. Tabata, and J. Silverman, *J. Chem. Phys.*, **61**, 3439 (1974).
(8) K. Kimura, M. Ogawa, M. Matsui, T. Karasawa, M. Imamura, Y. Tabata, and K. Oshima, *J. Chem. Phys.*, **63**, 1797 (1975).
(9) A. Henglein and W. Schnabel, "Current Topics in Radiation Research", Vol. II, M. Ebert and A. Howard, Ed., North-Holland Publishing Co., Amsterdam, 1966, p 52.
(10) O. Saito, *J. Phys. Soc. Jpn.*, **13**, 198 (1958); "The Radiation Chemistry of Macromolecules", Vol. I, M. Dole, Ed., Academic Press, New York, 1972, Chapter 11.
(11) A. R. Shultz, *J. Chem. Phys.*, **29**, 200 (1958).
(12) R. W. Kilb, *J. Phys. Chem.*, **63**, 1838 (1959).
(13) M. Inokuti, *J. Chem. Phys.*, **38**, 1174 (1963).
(14) A. M. Kotliar, *J. Polym. Sci., Part A*, **2**, 1057 (1964).
(15) G. G. Cameron, G. P. Kerr, and A. R. Gourlay, *J. Macromol. Sci., Chem.*, **2**, 761 (1968).
(16) D. I. C. Kells and J. E. Guillet, *J. Polym. Sci., Part A-2*, **7**, 1895 (1969).
(17) K. W. Scott, *J. Polym. Sci., Part C*, **46**, 321 (1974).
(18) T. L. Nemzek and J. E. Guillet, *Macromolecules*, **10**, 94 (1977).
(19) A. R. Shultz, P. I. Roth, and G. B. Rathmann, *J. Polym. Sci.*, **22**, 495 (1956).
(20) W. Burlant, D. Green, and C. Taylor, *J. Appl. Polym. Sci.*, **1**, 296 (1959).
(21) W. W. Parkinson, C. D. Bopp, D. Binder, and J. E. White, *J. Phys. Chem.*, **69**, 828 (1965).
(22) D. I. C. Kells, M. Koike, and J. E. Guillet, *J. Polym. Sci., Part A-1*, **6**, 595 (1968).
(23) M. Dole, "The Radiation Chemistry of Macromolecules", Vol. I, M. Dole, Ed., Academic Press, New York, 1972, Chapter 6.
(24) A. C. Ouano, D. E. Johnson, B. Dawson, and L. A. Pederson, *J. Polym. Sci., Polym. Chem. Ed.*, **14**, 701 (1976).
(25) W. Schnabel and H. Sotobayashi, *Polym. J.*, **8**, 423 (1976).
(26) J. N. Helbert, Chi-Yu Chen, C. U. Pittman, Jr., and G. L. Hagnauer, Macromolecules, **11**, 1104 (1978).
(27) K. Ishigure, S. Egusa, S. Tagawa, and Y. Tabata, 2nd International Meeting on Radiation Processing, Miami, Fla., October 1978; K. Ishigure, S. Egusa, M. Ogawa, S. Tagawa, and Y.

Tabata, *Polym. Prepr., Am. Chem. Soc., Div. Polym. Chem.*, **20**, 372 (1979).
(28) S. Egusa, K. Ishigure, and Y. Tabata, *Macromolecules*, submitted.
(29) S. An, T. Tamura, A. Furuhashi, and H. Wakabayashi, *Proc. Int. Symp. Phys. Fast Reactors*, **1**, 152 (1973).
(30) S. Egusa, K. Ishigure, S. Tagawa, Y. Tabata, and K. Oshima, *Radiat. Phys. Chem.*, 11, 129 (1978).
(31) J. Cazes and R. J. Dobbins, *J. Polym. Sci., Polym. Lett. Ed.*, **8**, 785 (1970).
(32) E. Cohn-Ginsberg, T. G. Fox, and H. F. Mason, *Polymer*, **3**, 97 (1962).
(33) C. J. Hochanadel, "Comparative Effects of Radiation", M. Burton, et al., Eds., Wiley, New York, 1960, p 174.
(34) G. Beck, D. Lindenau, and W. Schnabel, *Macromolecules*, **10**, 135 (1977).
(35) H. Yamakawa, M. Sakaguchi, and J. Sohma, *Rep. Prog. Polym. Phys. Jpn.*, **19**, 477 (1976).
(36) M. Tabata, K. Takahashi, H. Yamakawa, and J. Sohma, *Rep. Prog. Polym. Phys. Jpn.*, **20**, 531 (1977).
(37) A. Todd, *J. Polym. Sci.*, **42**, 223 (1960).
(38) C. David, D. Fuld, and G. Geuskens, *Makromol. Chem.*, **139**, 269 (1970).
(39) H. Hiraoka, *IBM J. Res. Dev.*, **21**, 121 (1977).

Dimensional Changes Accompanying the Formation of Poly(oxyethylene) Macrocycles

Wayne L. Mattice

Department of Chemistry, Louisiana State University, Baton Rouge, Louisiana 70803.
Received February 12, 1979

ABSTRACT: Cyclization of poly(oxyethylene) to form the macrocycle $3x$-crown-x, i.e., $(-CH_2CH_2O-)_x$, has been studied for even x from 4 to 20 using Monte-Carlo methods. Poly(oxyethylene) is assumed to behave in accord with the model developed by Mark and Flory. The fraction of acyclic chains satisfying criteria for cyclization reached a maximum of 1.2×10^{-3} for $x = 6$ and fell off to 0.1×10^{-3} when x was 20. The implication that 18-crown-6 is the most easily formed macrocycle is in harmony with experiment. Cyclization to form the larger macrocycles requires a reduction of $\langle L_1^2 \rangle$ by a factor of approximately 2, along with comparatively minor changes in $\langle L_2^2 \rangle$ and $\langle L_3^2 \rangle$. Here $L_1^2 \geq L_2^2 \geq L_3^2$ are the principal moments of the inertia tensor for the oxygen atoms, and angle brackets denote the average over all conformations. Cyclization to form crowns of the size investigated causes a reduction in the fraction of C–C bonds adopting trans placements. However, there is no significant change in the population of trans states at C–O bonds. The macrocycles 18-crown-6 and 24-crown-8 have definite preferences for certain spatial distributions of their oxygen atoms. Larger macrocycles are more flexible and show no great preference for a particular conformation. Among the most favored conformations for 18-crown-6 is the one seen in its complex with potassium ion. In contrast, metal-free 18-crown-6 crystallizes in a conformation which is occupied by only about 1% of the macrocycles in the unperturbed state.

Cyclization of moderately long chain molecules is an area of considerable current interest.[1] For example, a large variety of synthetic and naturally occurring macrocycles exhibit interesting ion-binding properties.[2-4] Many of these synthetic macrocycles consist wholely or in part of poly(oxyethylene).[2,5] As the size of a poly(oxyethylene) macrocycle increases, ring flexibility will eventually make it no longer profitable to attempt an explanation of molecular properties in terms of a small number of conformations. One current objective is to define the macrocycle size where this effect occurs for cyclic poly(oxyethylene). Especially favored conformations for smaller macrocycles will also be characterized. Finally, average conformation-dependent properties for both small and large macrocycles will be described, as well as changes in these properties accompanying cyclization. All calculations are based on a rotational isomeric state model[6-8] for unperturbed poly(oxyethylene) which is in harmony with measured unperturbed dimensions and dipole moments, as well as their temperature coefficients.

Calculational Method

Calculations are based on an adaptation of the macrocyclization theory utilized by Flory and co-workers.[9] It is conveniently described with the aid of Figure 1, which schematically depicts an acyclic $CH_3O(CH_2CH_2O)_xCH_3$ in a conformation nearly compatible with cyclization. The bond vector from chain atom $i-1$ to chain atom i is denoted $\mathbf{l}_i$. The initial CH_3–O bond is ignored in this numbering scheme, and the first oxygen atom is designated chain atom zero. The vector $\mathbf{r}$ is drawn from oxygen atom 0 to oxygen atom $3x$. Its length is zero in the cyclic molecule containing x oxygen atoms. (Such cyclic molecules are frequently denoted $3x$-crown-x.) Successful cyclization also requires the angle between $\mathbf{l}_1$ and $\mathbf{l}_{3x}$ be sufficiently close to the normal ∠C–O–C of 110°.

Representative chains were generated using the rotational isomeric state treatment developed by Mark and Flory[6,7] for poly(oxyethylene). Their treatment successfully accounts for experimentally observed unperturbed dimensions and dipole moments, as well as their temperature dependence. It has recently been used to account for an unusual temperature dependence in the NMR spectrum of certain poly(oxyethylene)macrocycles containing a 2,2′-bipyridyl subunit.[10] Chain geometry has bond lengths of 1.43 Å (C–O) and 1.53 Å (C–C), and bond angles are 110°. Three rotational states (trans, gauche$^{\pm}$) are available to each internal bond. Their dihedral angles are 0 and ±120°. Conditional and a priori probabilities were evaluated at 25 °C using the interaction energies assigned by Mark and Flory[6,7] and the appropriate rotational isomeric state formalism.[11] Conditional probabilities, in their matrix representation, are

$$\text{C–C bond} \quad \begin{bmatrix} 0.2050 & 0.3975 & 0.3975 \\ 0.2491 & 0.4832 & 0.2676 \\ 0.2491 & 0.2676 & 0.4832 \end{bmatrix} \tag{1}$$

$$\text{C–O bond} \quad \begin{bmatrix} 0.7247 & 0.1376 & 0.1376 \\ 0.7721 & 0.1466 & 0.0812 \\ 0.7721 & 0.0812 & 0.1466 \end{bmatrix} \tag{2}$$

$$\text{O–C bond} \quad \begin{bmatrix} 0.7352 & 0.1324 & 0.1324 \\ 0.8474 & 0.1526 & 0 \\ 0.8474 & 0 & 0.1526 \end{bmatrix} \tag{3}$$

Columns index the state of the bond in question, while

0024-9297/79/2212-0944$01.00/0